Reactive and Functional Polymers 196 (2024) 105842

Contents lists available at ScienceDirect

Reactive and Functional Polymers

journal homepage: www.elsevier.com/locate/react

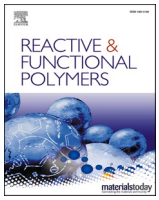

Hetero-functionalization of polyitaconates for developing improved polymer dielectrics: Merging sulfones with bulky/rigid cycles

Sebastian Bonardd [a,b,*], Jon Maiz [a,c], Angel Alegría [a,b], José A. Pomposo [a,b,c], Ester Verde Sesto [a,c], Galder Kortaberria [d], David Díaz Díaz [e,f]

[a] Centro de Física de Materiales (CSIC, UPV/EHU) and Materials Physics Center MPC, Paseo Manuel de Lardizábal 5, E-20018 Donostia, Spain
[b] Departamento de Polímeros y Materiales Avanzados: Física, Química y Tecnología, University of the Basque Country (UPV/EHU), Paseo Manuel de Lardizábal 3, E-20018 Donostia, Spain
[c] IKERBASQUE – Basque Foundation for Science, Plaza de Euskadi 5, 48009 Bilbao, Spain
[d] Materials + Technologies" Group, Chemical and Environmental Engineering Department, UPV/EHU, Plaza Europa 1, 20018 Donostia, Spain
[e] Departamento de Química Orgánica, Universidad de La Laguna, Avda. Astrofísico Francisco Sánchez 3, La Laguna 38206, Tenerife, Spain
[f] Instituto Universitario de Bio-Orgánica Antonio González, Universidad de La Laguna, Avda. Astrofísico Francisco Sánchez 2, La Laguna 38206, Tenerife, Spain

ARTICLE INFO

Keywords:
Polymer dielectrics
Dipolar glass polymers
Polyitaconates
Energy storage

ABSTRACT

This work addresses the preparation of new polymer dielectrics working under the *dipolar glass polymer* (DGP) concept. Herein, we report the synthesis and characterization of four hetero-functionalized polyitaconates bearing sulfones as high dipole moment entities and norbornane or adamantane structures responsible for increasing the glass transition temperature (T_g) and thus the range of temperatures where they can work without degrading or showing high energy dissipation. As a result, all obtained polymers exhibited dielectric constants (ε_r') between 5.1 and 6.2 while presenting low loss factors (Tan(δ) < 0.01), reaching the status of high-dielectric polymers with a low dissipative behavior. In addition, it was demonstrated that including bulky structures into their polymer backbone allows for an increase of up to 80 °C in their working temperature ranges, expanding the temperature range where they behave as DGPs in an outstanding manner. A complete structural, thermal and dielectric characterization was carried out in terms of infrared spectroscopy (FTIR), nuclear magnetic resonance (NMR), thermogravimetry (TGA), differential scanning calorimetry (DSC) and broad dielectric spectroscopy (BDS). Overall, these materials seem to fulfill the basic requirements to be considered good candidates for dielectric applications such as energy storage, confirming the versatility of polyitaconate-based materials.

1. Introduction

In the last decade, all-polymer dielectrics have garnered increasing attention from the scientific community, resulting in an abrupt increase research interest [1–8]. As a consequence, the amount and diversity of new polymer materials with enhanced dielectric properties have shown a remarkable increase. This allows not only the development of new materials but also enriches our understanding of the topic from a theoretical perspective, which, in any case, reinforces the former [9–11]. Arguably, the sudden interest in the field can be attributed to the energy situation our current society is facing. Without changing our consumption habits and the sources from which we obtain energy, an upcoming energy shortage is inevitable [12]. Therefore, it is imperative to grasp that the development of efficient and sustainable energy acquisition processes from clean and renewable sources would be in vain if, once obtained, we are unable to utilize it effectively. To ensure this, one approach involves creating and/or reinforcing technologies that focus on efficient storage, conversion and distribution of obtained energy. This is where polymer dielectrics emerge as attractive candidates to achieve and promote a more efficient and effective energy storage process, particularly through the fabrication of improved capacitor devices [6,13–15].

A capacitor allows energy storage in the form of electrostatic energy that, subsequently, can be released as electrical discharge. These devices find application in a wide spectrum of areas ranging from trivial electrical circuits (such as household appliances and defibrillators, among

* Corresponding author at: Centro de Física de Materiales (CSIC, UPV/EHU) and Materials Physics Center MPC, Paseo Manuel de Lardizábal 5, E-20018 Donostia, Spain.
E-mail address: sebastianignacio.bonardd@ehu.eus (S. Bonardd).

https://doi.org/10.1016/j.reactfunctpolym.2024.105842
Received 20 November 2023; Received in revised form 25 January 2024; Accepted 26 January 2024
Available online 1 February 2024

others) to other more complex and advanced ones such as power pulse applications, hybrid/electric vehicles, aerospace technology, robotics, (bio)sensors, rectifiers and accumulators in wind and solar farms [3,6,16]. The heart of a capacitor is, precisely, the dielectric material, which is intimately related to the amount of charge (energy) that the device is able to store. Therefore, physics has taught us that the maximum energy stored that a capacitor could sustain follows the relation $U_e = ½(\varepsilon_r' E_b^2)$, where ε_r' and E_b represent the dielectric constant and dielectric breakdown, respectively [3]. Both parameters are directly related to the dielectric material placed in the capacitor, evidencing the need to employ materials with the highest possible ε_r' and E_b values. Regarding the above, using polymers as dielectrics presents advantages and disadvantages when compared, for example, to inorganic systems. Among the advantages, probably the most relevant, is that polymers offer notably higher E_b values as dielectric media, in addition to their better mechanical properties, light weight, easy processability and manufacture, synthetic versatility and low-cost production. However, they lack high ε_r' values, usually falling within the range of 2–4 [3,17]. Unfortunately, E_b – which is the one contributing more from a mathematical point of view – has shown a tighter relationship with the inherent nature of the material, making it difficult to modify while on the contrary, ε_r' has been shown to be more tunable by manipulating the chemistry of the material. Taking into account the above, it has been demonstrated that by endowing a material with a greater polarization ability, its ε_r' can be augmented outstandingly [18,19]. Therefore, searching for new strategies to afford the preparation of polymers with ε_r' above conventional values but also presenting a low dissipative behavior has become a demanded and fruitful research field.

Regarding the latter, to date, one of the most effective and promising strategies for developing new polymer dielectrics with high ε_r' and low dissipation behavior is the manufacture of *dipolar glass polymers* (DGPs). This concept, introduced by Lei Zhu [17] almost ten years ago, is referred to as polymeric materials fulfilling two main requirements: 1) to contain small-sized high dipole moment functional groups covalently attached to its structure and 2) to be an amorphous material with a glass transition temperature (T_g) as high as possible [20]. Therefore, the polarization mechanism through which DGPs base their dielectric properties is mainly governed by the orientational motions that these dipolar entities can perform within the amorphous matrix when exposed to an external electric field. In this context, the need for an amorphous structure is driven by the inherent free volume present in these materials. This, combined with the requirement for small-sized dipole moment functional groups, creates an environment conducive to unhindered orientational motions. Equally crucial is the demand for a high T_g, ensuring the material's resilience under the typically heated conditions experienced by dielectric materials.

A high T_g value serves a dual purpose. First, it prevents the material from entering a rubbery state that could lead to leakage and subsequent failure. Second, it delays the onset of dissipative phenomena on the temperature scale, directly influencing the energy storage capacity of the system. Among various dissipative phenomena, the rise in ionic conductivity near T_g is particularly detrimental, as it impacts the insulation property of the dielectric material [18,20,21]. This is a consequence of diffusion processes facilitated by ionic impurities, which are inherently present in these polymeric materials and become activated as the polymer chains undergo long segmental motions, typically occurring when the material approaches its rubbery state. When a DGP surpasses its T_g, it transitions into a *paraelectric* state characterized by higher polarization but also a highly dissipative behavior. Ideally, in a DGP, one seeks a material with dipolar structures capable of orientational motions from the lowest possible temperature while also possessing the highest attainable T_g value. This would result in a material exhibiting a wide temperature range with a highly polarized state, devoid of significant dissipative processes. This temperature range, often referred to as the DGP's `sweet spot', represents the regime where the *paraelectric* state dominates [22].

The large number of reports within the last five years demonstrates the success of DGPs as a strategy for the preparation of new all-polymer dielectrics with high ε_r' values (> 4) [8,23–26]. In this sense, diverse polymer structures ranging from aromatic to aliphatic and from synthetic to bio-based systems have been designed and prepared to contain highly dipolar functionalities and achieve superior dielectric properties [4,26–32]. Among these functionalities, nitriles and sulfones have been the ones that have attracted the most attention due to their high dipole moments (3.9 and 4.25 Debye, respectively) and easy incorporation [17]. However, in 2015, Wei et al. set an unprecedented result in the field of DGPs, where a new sulfonyl-containing polymethacrylate achieved an ε_r' value of 11.2 and a loss factor – Tan(δ) – of 0.02 at room temperature [20]. Since then, sulfones have taken the lead as dipolar entities for excellence in developing new polymer materials with improved dielectric properties, as can be verified in the following references to name a few [22,33–41]. Of course, it is evident that one of the paths to follow in seeking new and improved DGPs is the design and testing of new polymer structures decorated with these molecular dipoles. In this context, and fortunately, some of us were able to contribute to this field by introducing, for the first time, polyitaconates as dielectric media [34,42,43]. One of the main attractiveness of these polymers is the double functionality of their monomeric units – derived from itaconic acid – that permits playing not only with the type of substituent but also with the number, in this case, of dipoles. Thus, in a series of consecutive works, we have successfully proven that these materials can act as valuable dielectric media by exhibiting high ε_r' values (from 4 to 16) while presenting low Tan(δ) values (< 0.02) after the chemical incorporation of nitriles and sulfonyl groups. More importantly, we have also demonstrated that the incorporation of bulky pendant groups into dipole-containing polyitaconates turned out to be a suitable strategy to dramatically increase the T_g of these systems and, consequently, the temperature range where these behave as DGPs.

Thus, with the aim of continuing to explore the performance of polyitaconates as dielectric media, this work presents a novel approach to achieve an improved version of our previous report dealing with the use of dipolar polyitaconates bearing bulky substituents [43]. In that opportunity, we successfully prepared of three new polyitaconates hetero-functionalized that had, on the one hand, norbornane or adamantane pendant groups and, on the other hand, nitriles as dipolar entities. Even when these materials exhibited notably high T_gs, broad DGP temperature ranges and, therefore, low dissipative behavior (Tan <0.01), their ε_r' values – between 4.0 and 4.3 – barely surpassed the upper limit established for conventional polymers. Therefore, to reach higher ε_r' values and inspired by the superior performance shown by sulfonyl-containing polymers, in this work we carried out for the first time the replacement of nitriles by sulfone units in four new polyitaconates having norbornane and adamantane derivatives as secondary pendant groups. These materials were successfully prepared through the polymerization of their respective monomeric units and characterized in terms of their structural, thermal, and dielectric properties.

2. Experimental section

2.1. Materials

Itaconic acid (≥ 99%, CAS 97–65-4), acetyl chloride (≥ 99%, CAS 75–36-5), Exo-norborneol (98%, CAS 497–37-0), 2-Norbornanemethanol (mixture of endo and exo, 97%, CAS 5240-72-2), 1-Adamantanemethanol (99%, CAS 770–71-8), 1-Adamantanol (99%, CAS 768–95-6), *N,N′*-dicyclohexylcarbodiimide (DCC, 98%, CAS 538–75-0), and 4-(dimethylamino)pyridine (DMAP, ≥ 99%, CAS 1122-58-3) were all purchased from Sigma–Aldrich. 2-(Methylsulfonyl)ethanol (98%, CAS 15205–66-0) was acquired from Fluorochem. 2,2′-Azobis(2-methylpropionitrile) (AIBN, 98%, CAS 78–67-1) was purchased from Fluka. All solvents used in this work were purchased from Merck and used without further purification unless stated.

2.2. Characterization techniques

^{1}H NMR and ^{13}C NMR spectra were recorded on a Bruker Avance II-500 system using $CDCl_3$ and DMSO-d_6 as solvents for monomers and polymers, respectively. FTIR spectra of specimens were recorded in a Cary 630 FTIR spectrophotometer (Agilent) equipped with an ATR accessory between 650 and 4000 cm^{-1} after 34 scans in transmission mode and with a resolution of 2 cm^{-1}. The molecular weight of polymers was determined by size-exclusion chromatography (SEC) using a Shimadzu Nexera 40 HPLC system, equipped with a polar gel-M guard (50 × 7.5 mm) and a polar gel-M column (300 × 7.5 mm), both from Agilent. A differential refractive index (dRI) detector (RID-20 A, Shimadzu) was used as a detection system. A solution of LiBr in *N,N*-dimethylformamide (DMF) (0.1 wt%) was used as the eluent (1 mL/min flow rate), and polystyrene (PS) standards were employed for conventional calibration. The density values of the polymer films were calculated using a top-loading electronic METTLER balance (ME-33360) and methanol (density 0.792 g/cm^3 at room temperature).

The thermal characterization of samples was carried out using a simultaneous thermal analyzer (TG/DSC) Discovery SDT 650 (TA Instruments) and a differential scanning calorimeter Discovery DSC 025 (TA Instruments). Thermogravimetric analysis (TGA) was performed between 25 °C and 800 °C at 10 °C/min under a nitrogen atmosphere. From the obtained thermograms, the degradation onset temperature (T_i), maximum weight loss rate temperature (T_{MD}) and residue percentage (R) were calculated. T_i is defined as the temperature at which the material loses 5% of its initial weight. On the other hand, differential scanning calorimetry (DSC) analysis involved the following five consecutive steps: i) dynamic heating from 25 °C to 200 °C at 20°/min, ii) isothermal process at 200 °C for 3 min, iii) dynamic cooling process going from 200 °C to 0 °C at 20 °C/min, iv) isothermal process at 0 °C for 3 min, and finally, v) a dynamic heating process from 0 °C to 200 °C at 10°/min. The informed glass transition temperatures (T_g) were calculated from the inflection point detected in thermograms acquired from the last heating step.

Broadband dielectric spectroscopy was used to perform the dielectric characterization of the materials. Measurements were carried out using a Novocontrol Alpha high-resolution analyzer with an applied AC voltage of 1.0 *V*, from which frequency scans (isothermal spectra) and temperature scans (isochronal spectra) were obtained. Frequency scans were measured in the range between 10^{-1} and 10^{6} Hz. These measurements were taken at different temperatures ranging from – 150 °C to 25 °C. On the other hand, isochronal spectra were recorded from – 150 °C to 150 °C at frequencies between 1 and 10^{6} Hz. The sample preparation for dielectric measurements is outlined below. First, a certain amount of polymer powder is hot-pressed between two metal discs at a temperature T_g + 30 °C and 2 tons of pressure, achieving the formation of a bubble-free film. Later, this film was hot-pressed again between two gold-plated electrodes of different diameters (20 mm and 30 mm), using the electrode with the greater diameter as the bottom part in the sandwich configuration. Initially, the thickness of the film was determined as the difference in thickness between both electrodes before and after hot pressing the polymer film. However, the above value was corrected by measuring the thickness of the peeled-off film from the electrodes after the dielectric measurements. It is worth mentioning that samples placed between electrodes were dried overnight under vacuum at 130 °C and then stored in a desiccator before analysis. Relative permittivity values (ε_r') were calculated using eq. 1:

$$\varepsilon'_r = \frac{C_p' d}{\varepsilon_O \pi r^2} \quad (1)$$

where ε_r' is the calculated dielectric constant, C_p' is the real part of the measured capacitance in the parallel configuration, *d* is the thickness of the polymer film, $\varepsilon_{o\ is}$ the vacuum permittivity (8.85×10^{-12} F m^{-1}) and *r* is the radius of the top electrode. Once calculated ε_r', the dielectric loss (ε_r") parameter was calculated using the relation $\varepsilon_r" = \varepsilon_r'$ Tan(δ), where Tan(δ) is the loss factor obtained directly from the experimental measurements.

A Metricon model 2010 prism coupler was used to determine the refraction index (*n*) of the polymer films after dielectric measurements. Values of 1.5285, 1.5292, 1.5298, and 1.5304 were obtained for PSO_2mNORI, PSO_2NORI, PSO_2mADAI and PSO_2ADAI, respectively.

2.3. Monomer synthesis

The spectroscopic data (FTIR, ^{1}H and ^{13}C NMR) belonging to itaconic anhydride, the obtained monomers and their respective intermediates can be consulted in the supporting information file.

2.3.1. Itaconic anhydride

In a two-neck round bottom glass, 10 g (7.7 mmol) of itaconic acid and 19 mL (26.3 mmol) of acetyl chloride were added and stirred at 55 °C for 2.5 h. Then, 10 mL of dry toluene was added to the reaction and refluxed for 3 h using a Dean-Stark apparatus. Subsequently, 25 mL of diethyl ether was added, and the solution was stored at −20 °C overnight. The resulting white crystals were washed with cold diethyl ether and dried in a vacuum oven until constant weight. Yield: 81%. Melting point: 65–68 °C.

2.3.2. Preparation of mono methylnorbornyl itaconic acid (1a), mono norbornyl itaconic acid (1b), mono methyladamantyl itaconic acid (1c) and mono adamantyl itaconic acid (1d)

The synthesis of mono-ester itaconic acids **1a**, **1b** and **1c** was achieved following a slightly modified protocol previously reported by our group, which was also useful for the preparation, for the first time, of specimen **1d** [43]. Briefly, in a two-neck round bottom flask coupled to a reflux system, 2.00 g (18 mmol) of itaconic anhydride was mixed with 1.2 equivalents (21 mmol) of the corresponding alcohol and solubilized in 15 mL of dry toluene. The reaction was heated at 120 °C for 24 h, after which the solvent was removed in a rotary evaporator at reduced pressure, obtaining a transparent oil in all cases. **1a** and **1b** were successfully purified by crystallization, pouring the transparent oil into 10 mL of hexane and storing them for 24 h at −20 °C, allowing the formation of white crystals. In the case of **1c** and **1d**, the purification process was carried out by column chromatography using a mixture of hexane:acetone (7:3) as the eluent, to give a transparent oil that solidifies in the form of white crystals upon cooling at −20 °C. Samples **1a**, **1b**, **1c** and **1d** were obtained with yields of 68, 81, 55 and 57%, respectively.

2.3.3. Preparation of 2-(methylsulfonyl)ethyl methylnorbornyl itaconate (2a), 2-methylsulfonylethyl norbornyl itaconate (2b), 2-methylsulfonylethyl methyladamantyl itaconate (2c) and 2-methylsulfonylethyl adamantyl itaconate (2d)

The synthesis of diitaconates **2a**, **2b**, **2c** and **2d** was performed starting from their corresponding mono itaconate esters **1a**, **1b**, **1c** and **1d**, following the same experimental protocol in each case. The protocol is described below, using the synthesis of **2a** as an example:

A total of 3.0 g of **1a** (13.0 mmol) and 2.4 g of 2-(methylsulfonyl) ethanol (19.5 mmol, 1.5 equiv) were solubilized in 30 mL of dry dichloromethane (DCM) and cooled in an ice-water bath. Simultaneously, a second solution was prepared in a round-bottom glass by dissolving 3.2 g of DCC (15.6 mmol, 1.2 equiv) and 0.3 g of DMAP (2.6 mmol, 0.2 equiv) in 70 mL of dry DCM, which was left under constant stirring in an ice-water bath. Afterwards, when both solutions reached 0 °C, the first solution was added dropwise over the second solution under constant stirring, and after concluding the addition, the reaction mixture was allowed to reach room temperature and react for 24 h, maintaining the stirring conditions. Then, the mixture was stored overnight at −20 °C to favor the precipitation of the dicyclohexyl urea (DCU) subproduct. The cooled mixture was filtered and subjected to

consecutive washing steps with brine (5 × 50 mL), after which the organic phase was dried over anhydrous $MgSO_4$ and filtered. The solvents were removed under reduced pressure, and the whitish oil obtained (with clear presence of DCU traces) was successfully purified by column chromatography (7:3, ethyl acetate:hexane), affording a transparent oil that slowly formed a white solid over time (**2a**). Yield = 71%.

Similarly, after column chromatography, **2b**, **2c** and **2d** turned out to be transparent oils that, after a certain period of time, became white solids. The calculated yields for **2b**, **2c** and **2d** were 68, 61 and 78%, respectively.

2.4. Synthesis of polyitaconates

The synthesis of polymers was carried out in bulk using AIBN as the radical initiator. Typically, 2.0 g of monomer was placed into a Schlenk tube equipped with a magnetic stirrer, followed by the addition of the respective amount of AIBN to afford an initiator concentration of 0.5 mol%. The system was subjected to three consecutive freeze–thaw cycles employing liquid nitrogen and finally purged with dry N_2. The entire system was immersed in an oil bath thermostated at 70 °C and stirred for 48 h. After completing the reaction time, the mixture was exposed to air, dissolved in 10 mL of *N,N′*-dimethylformamide (DMF), precipitated into 150 mL of methanol and filtered. The above process was repeated three times. Finally, the obtained white powders were dried at 120 °C in a vacuum oven for 72 h prior to characterization. The nomenclature chosen for the obtained polymers was PSO_2mNORI, PSO_2NORI, PSO_2mADAI and PSO_2ADAI, which were obtained directly from the polymerization of monomers **2a**, **2b**, **2c** and **2d**, respectively. Conversion values of 72%, 64%, 58% and 50% were calculated for PSO_2mNORI, PSO_2NORI, PSO_2mADAI and PSO_2ADAI, respectively.

3. Results and discussion

The experimental part of the present project began with the design and preparation of the corresponding monomers that would allow the obtainment of this new family of polyitaconates. Scheme 1 illustrates the synthetic route employed to achieve the preparation of the devised monomers **2a**, **2b**, **2c** and **2d**.

All monomers were derived from itaconic anhydride (**1**), which was successfully synthesized from itaconic acid using well-established methods [43]. Subsequently, this anhydride was reacted under reflux conditions with the corresponding alcohols derived from norbornane and adamantane structures. This induced the opening of the anhydride structure, leading to the formation of mono itaconate esters **1a**, **1b**, **1c** and **1d** in yields ranging from regular to good. This was confirmed by ^1H and ^{13}C NMR analysis (Figs. S1 – S5). Subsequently, each monoester underwent a second esterification process using the Steglich protocol. [44] This led to the incorporation of sulfone entities into the final monomeric structures, resulting in the obtainment of diitaconates **2a**, **2b**, **2c** and **2d.** This was also confirmed by ^1H and ^{13}C NMR analysis (Figs. S6 – S9). Importantly, all diitaconates were successfully polymerized using conventional radical polymerization under bulk conditions, as depicted in Scheme 2.

These polyitaconates, all containing sulfonyl groups as high dipole moment entities, can be categorized into two families based on the structure of the attached aliphatic cycle. In this sense, one family would be represented by PSO_2mNORI and PSO_2NORI, having norbornane-like structures, with the only structural difference between them being the

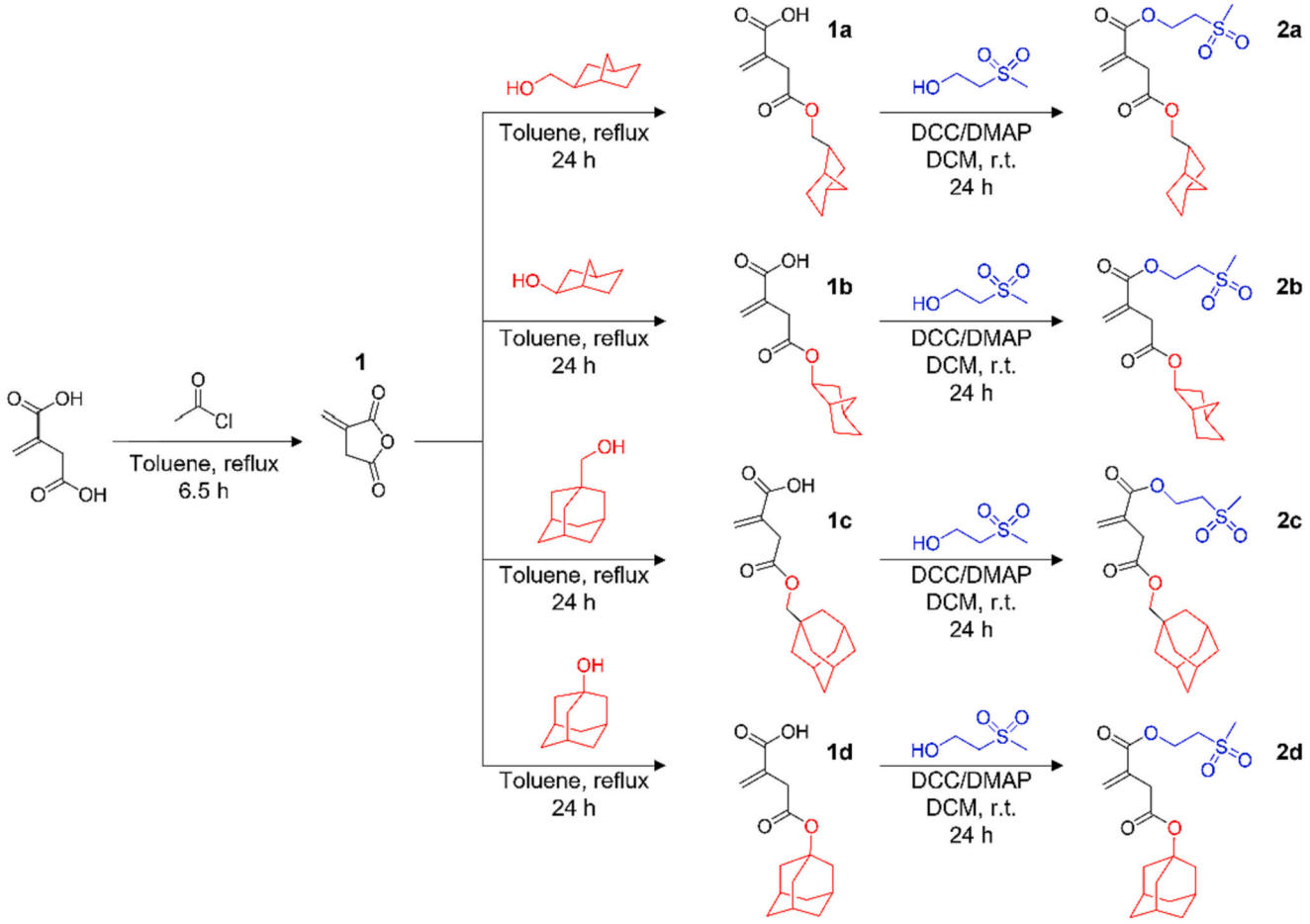

Scheme 1. Synthetic route for obtaining hetero – functionalized itaconate monomers.

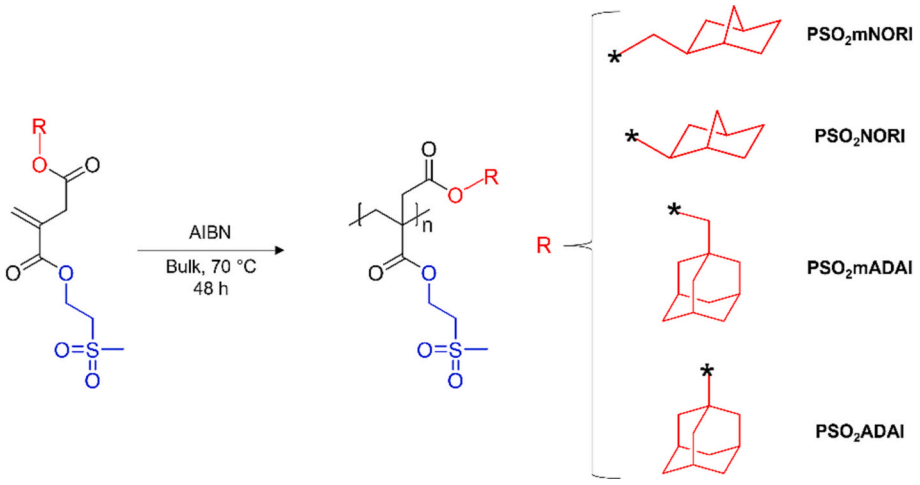

Scheme 2. Preparation of sulfonyl-containing polyitaconates through bulk radical polymerization.

presence of a methylene spacer unit in PSO_2mNORI. Likewise, the second family includes PSO_2mADAI and PSO_2ADAI, both featuring adamantane-based moieties. Once more, the primary structural distinction between them lies in the presence of the methylene unit in PSO_2mADAI. The conversion values for all obtained polymers were in the range of 50–72%. Interestingly, when comparing within the same family, systems with the spacer unit exhibited higher conversion values. Conversely, comparing specimens with or without the spacer unit revealed that those bearing norbornane groups also exhibited higher conversions than those with adamantyl pendant groups. This can be attributed to the higher steric hindrance generated: 1) the absence of the methylene spacer unit, bringing the aliphatic cycle closer to the polymerizable section of the monomer, and 2) the replacement of norbornane structures by bulkier adamantane entities. [45–48]

The structural characterization of these polyitaconates was first addressed through FTIR analysis, where spectra of the obtained polymers are displayed in Fig. 1.

The FTIR analysis revealed very similar spectra among the four

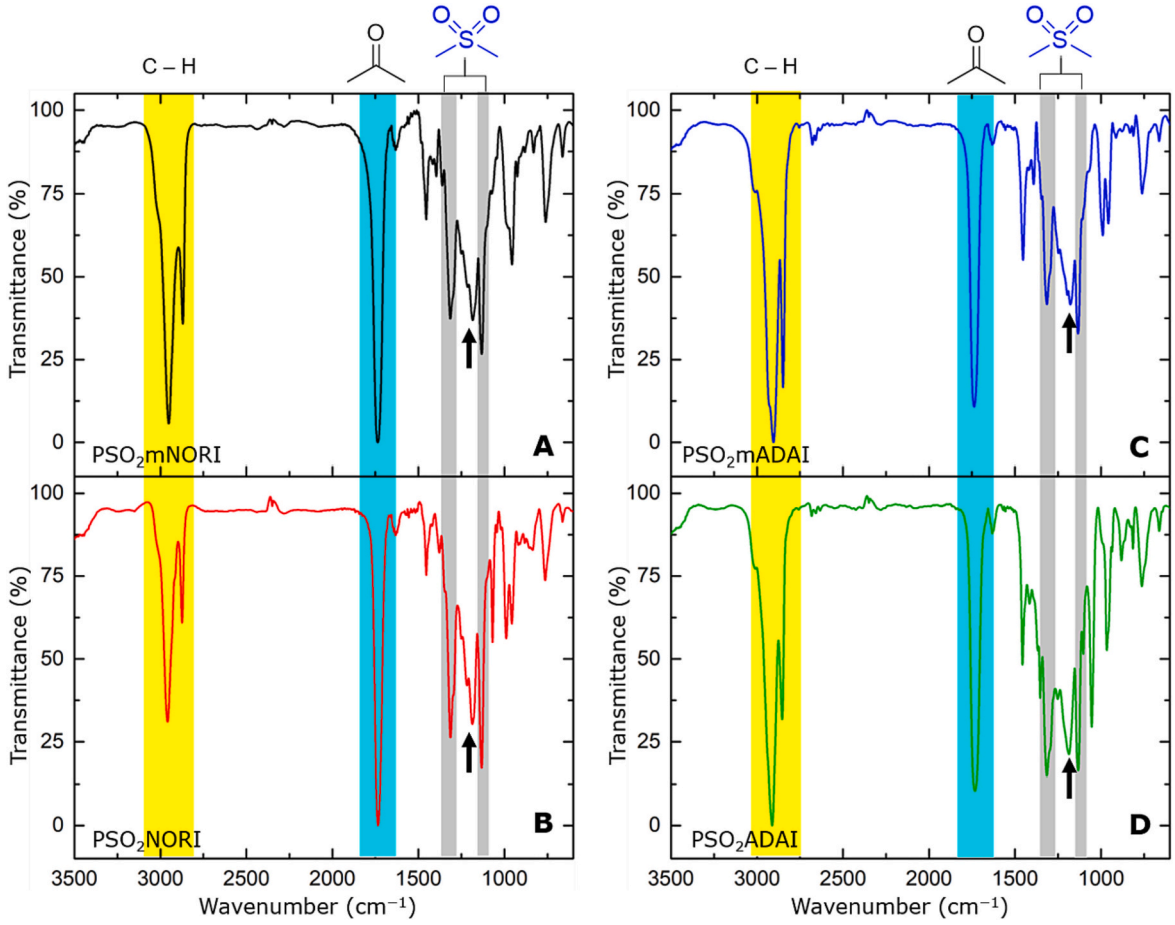

Fig. 1. FTIR spectra recorded for PSO_2mNORI (A), PSO_2NORI (B), PSO_2mADAI (C) and PSO_2ADAI (D).

specimens, which was anticipated due to the notable similarities in their chemical structures. In light of this, three colored regions were highlighted in all spectra to identify the groups of signals that would confirm the presence of the desired functionalities. The yellow zone, defined between 3000 and 2800 cm^{-1}, encompasses two vibrational bands arising from the C – H linkages originating from the aliphatic content in the polymer backbone. Additionally, it includes a significant contribution of –CH– and – CH_2– units belonging to norbornane and adamantane pendant structures. Indeed, this group of signals stands out by their remarkable intensities, being the most intense in the PSO_2mADAI and PSO_2ADAI spectra due to the presence of adamantane units. Interestingly, the second band appearing at lower wavenumber values (~2860 cm^{-1}) has been previously assigned to certain vibrational modes of C – H linkages present in this class of rigid cycles [49]. At lower wavenumber values, within the cyan zone, an intense and sharp signal centered around ~ 1735 cm^{-1} would accuse the presence of the typical carbonyl structures of polyitaconates. Crucially, the presence of sulfone groups was confirmed by identifying the two characteristic bands of this dipolar entity centered at ~ 1315 cm^{-1} and ~ 1132 cm^{-1} (highlighted in gray), corresponding to the symmetric and asymmetric stretching motions of these functionalities, respectively [50]. Finally, indicated by black arrows, a signal centered at approximately 1180 cm^{-1} can be identified in all spectra. This corresponds to the vibrational motions of C – O – C linkages that are part of the ester groups present in the monomeric units of these materials. As a complement to the FTIR analysis, the chemical structure of these polymers was also studied by ^{1}H and ^{13}C NMR, and the results are shown in Fig. 2 and Fig. S10, respectively.

NMR analysis of the four obtained polymers successfully identified distinct fragments belonging to their respective monomeric structures. In this context, the presence of sulfonyl-containing structures (blue fragments in Fig. 2) was discerned in all ^{1}H NMR spectra. This was primarily accomplished by identifying the methylene units from the 2-methylsulfonyl ethyl pendant groups. More notably, the characteristic signal attributed to the methyl group directly attached to the sulfonyl moiety provided crucial confirmation. Conversely, the presence of norbornane or adamantane structures (red fragments in Fig. 2) is substantiated by the multitude of densely packed signals appearing at high field. These signals exhibit significant intensity and a notable degree of overlap, making it difficult to assess the main-chain protons labeled as 1 and 2, which should appear in the range between 3.0 and 2.0 ppm as evidenced in previous polyitaconate systems. Additionally, these signals tend to exhibit a low intensity and definition due to tacticity phenomena, affecting their visualization. [34,42,43,51] Similarly, the analysis of ^{13}C NMR spectra – shown in Fig. S11 – corroborates the previously extracted information. Successful signal assignment for the various carbon nuclei was accomplished, with the exception of certain main-chain carbon atoms (e.g., carbon C), likely due to its overlap with the DMSO solvent signal. Thus, by complementing the FTIR and NMR analyses, the structure of the obtained polymers can be confirmed. Therefore, once demonstrated, their macromolecular nature was

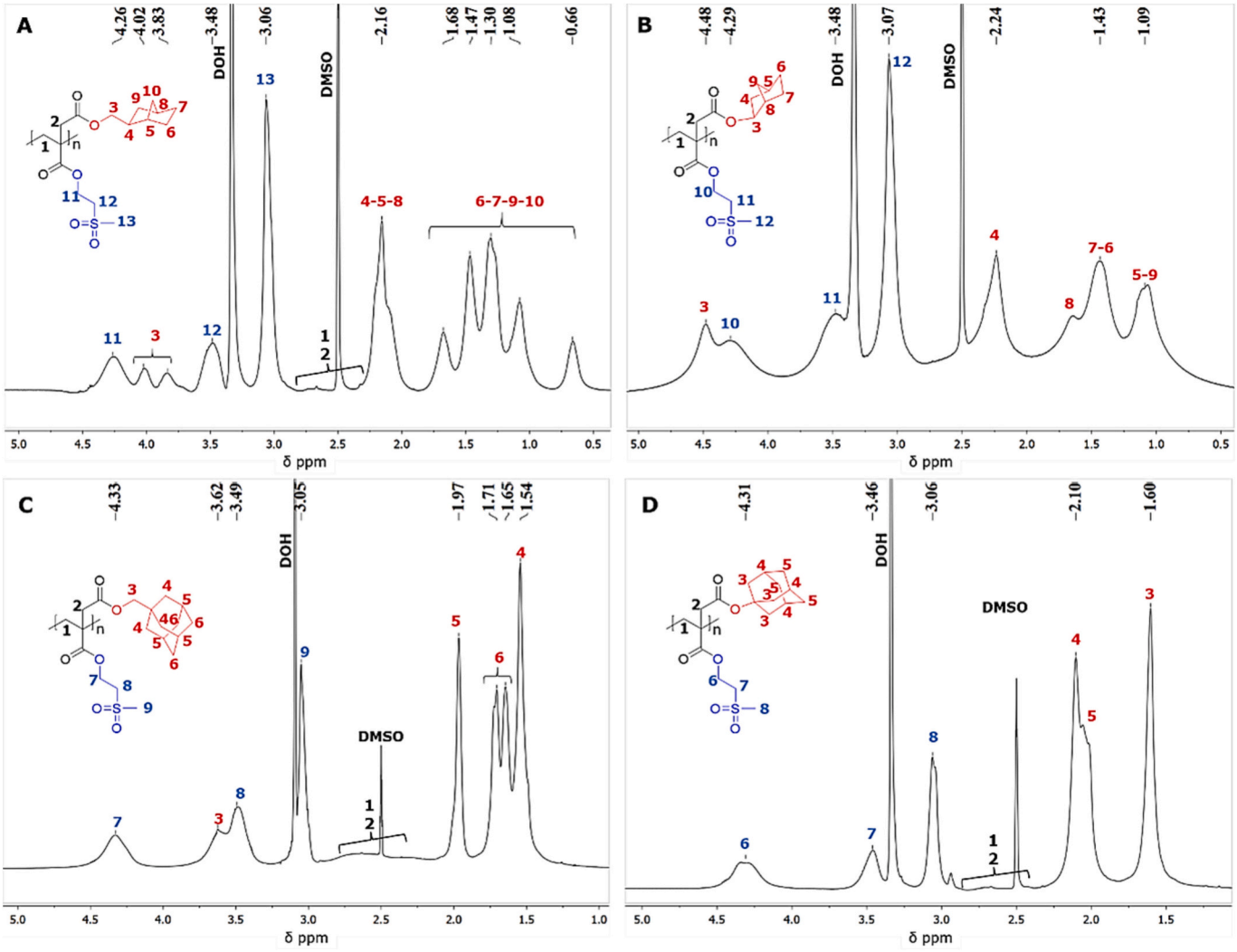

Fig. 2. ^{1}H NMR spectra registered for PSO_2mNORI (A), PSO_2NORI (B), PSO_2mADAI (C) and PSO_2ADAI (D).

confirmed by gel permeation chromatography (GPC), through which their average molecular weights, along with their dispersity indexes (Đ), were obtained. The results are summarized in Table 1.

The molecular weights obtained for PSO_2mNORI, PSO_2NORI and PSO_2mADAI correlate well with our previous reports on the preparation of counterparts bearing nitrile groups as dipolar entities [43]. An exception arises with PSO_2ADAI, which exhibits a molecular weight value approximately one order of magnitude lower. Overall, considering the experimental conditions employed during the polymerization step, the obtained values are significantly lower than those reported in previous studies concerning the preparation of other polyitaconate materials [43,45]. We believe that the incorporation of norbornane and adamantane groups into the monomeric units significantly affects their addition/reactivity toward the terminal radicals of growing chains, and the main argument supporting this should be the increased steric hindrance that these monomers expose due to the presence of these bulky structures. Based on the above, it could be suggested that the lower molecular weight of PSO_2ADAI may be attributed to its monomer unit, which, among all tested monomers, presents the highest steric hindrance. Conversely, concerning the Đ values, all of them fall within the anticipated range for this type of conventional radical polymerization. It should be noted that, in accordance with previous studies the average molecular weight and dispersity values exhibited by these types of materials should not substantially affect their polarization properties [20,52]. This is because the polarization phenomena of *dipolar glass polymers* primarily depend on the local movements of dipolar structures rather than long-range motions.

The thermal properties of these new polyitaconates were evaluated in terms of TGA and DSC analyses, and the results are shown in Fig. 3 and summarized in Table 2.

TGA analysis reveals that all samples exhibit remarkably similar degradation profiles (Figs. 3 A – D), with two discernible degradation steps characterized by temperatures T_{MD1} and T_{MD2}. It is important to note that, in all cases, >80% of the mass loss occurs during the first step. Arguably, various phenomena occurring simultaneously within the temperature range initiate the cleavage of chemical bonds present in the materials. This could be brought about by the cleavage of pendant groups or even the random fragmentation of the polymer backbone, leading to the generation of radical species that, under these high temperature conditions, can initiate depolymerization processes. In this sense, low molecular weight species would be generated and volatilized as degradation products. Similarly, albeit with a significantly lower mass contribution, the second step may be associated with the degradation of certain chemical structures that persist after the first step. However, the thermal stability of these materials is better characterized by the onset degradation temperature (T_i), defined in this case as the temperature at which the material loses 5% of its initial weight. Based on the above, it is evident that all the obtained polyitaconates commence degradation well above 250 °C, a condition established to deem as materials possessing adequate high-thermal resistance for application as dielectric media [16]. In line with our previous report on bulky polyitaconates [43], it is evident once again that the materials with monomeric structures lacking methylene spacer units (PSO_2NORI and PSO_2ADAI) exhibited lower T_i and T_{MD1} values than their counterparts, PSO_2mNORI and PSO_2mADAI (Table 2). This lower thermal resistance has been previously attributed to a possibly more rigid structure that would result in a less stable system against bond vibrations induced by thermal energy. Importantly, these samples possess a markedly higher thermal stability than PSO_2MeiT (T_i = 277 °C), a dipolar glass polymer previously reported by us, consisting of a sulfone-containing polyitaconate obtained after the replacement of norbornane/adamantane structures by methyl units [34].

In DSC analysis, as shown in Fig. 3E, it is evident that all obtained polymers display an amorphous behavior, completely devoid of crystallization/melting phenomena. This fulfills a crucial criterion for defining them as *dipolar glass polymers*. Furthermore, these materials distinguish themselves by exhibiting glass transition temperatures (T_g, indicated by black arrows) well above room temperature, surpassing the 100 °C threshold (Table 2). The elevated T_g values can be attributed to the presence of norbornane/adamantane structures, which, owing to their bulkiness and rigid nature, augment the rigidity of the macromolecular structures. Experimentally, the role of these cyclic entities in elevating T_g was demonstrated by comparing these results with the T_g value of PSO_2MeiT, reported at 101 °C, even though the latter exhibited a significantly higher molecular weight [34]. Another intriguing observation arises when comparing the T_g values between PSO_2mNORI and PSO_2NORI, where a notable increase of approximately 32 °C was achieved by simply removing the methylene spacer unit between the norbornane structure and the polymer backbone. This could be attributed to a potentially favorable contribution to the free volume within the system that these spacer units could offer, where the absence of these CH_2 units would decrease the degrees of freedom of the bulky pendant groups, restricting their possibility to achieve different spatial orientations within the material's structure. On the contrary, for PSO2mNORI, the greater orientational dispositions available for the norbornane structures could favor an increment of the free volume in the material, resulting in a lower T_g value. Unexpectedly, this trend was not observed in the case of PSO_2mADAI and PSO_2ADAI, likely due to the markedly lower molecular weight exhibited by PSO_2ADAI since, as is well known, there is a close dependence between T_g and molecular weight in polymeric materials. [53,54] Nevertheless, this suggests that in the event of successfully preparing a PSO_2ADAI specimen with an increased molecular weight, significantly higher T_g values could be anticipated. Finally, as a noteworthy trend, when comparing these polymers with their counterparts featuring nitrile groups as dipolar entities, the former exhibited higher T_g values. Considering that molecular weight values are on the same order of magnitude, the above result could be related to stronger dipolar interactions within the sulfone-containing specimens. This could also be reflected in the higher-density values that the sulfone-bearing systems exhibited against those with nitrile moieties [34]. In this context, density values of 1.28, 1.24, 1.22 and 1.20 g/cm^3 were obtained for PSO_2mNORI, PSO_2NORI, PSO_2mADAI and PSO_2ADAI, respectively.

After completing the thermal characterization of these materials, their dielectric properties were evaluated in terms of BDS measurements. Fig. 4 displays isochronal measurements of the dielectric constant (ε_r'), dielectric loss (ε_r") and loss factor (Tan(δ)) parameters at different frequencies and temperatures for all obtained polyitaconates.

Isochronal representations are particularly useful for directly observing how ε_r', ε_r" and Tan(δ) parameters vary with changes in frequency and temperature. Importantly, they facilitate the visual assessment of any relaxation phenomena occurring in the material as temperature varies. It is worth noting that all obtained polymers exhibit a similar dielectric response characterized by closely matching profiles ε_r', ε_r" and Tan(δ). This outcome was anticipated due to the structural similarities between them. Regarding the dielectric constant, a qualitative inspection of ε_r' profiles reveals an increase in this parameter as the temperature rises. This corresponds well with the thermal activation needed for dipolar entities to overcome the potential energy barriers imposed by their surroundings [55,56]. This increase is marked by two distinct jumps: the first occurring at low temperatures (approximately –100 °C) and the second becoming apparent from ~ 100 °C onwards. It is noteworthy that between these jumps, a slight but consistent rise in ε_r' is

Table 1
Number (M_n) and weight (M_w) average molecular weights along with dispersity values (Đ) of synthesized polymers.

	PSO_2mNORI	PSO_2NORI	PSO_2mADAI	PSO_2ADAI
M_n (g/mol)	1.23×10^4	2.99×10^4	3.10×10^4	3.08×10^3
M_w (g/mol)	2.29×10^4	6.05×10^4	6.07×10^4	4.43×10^3
Đ	1.86	2.02	1.96	1.44

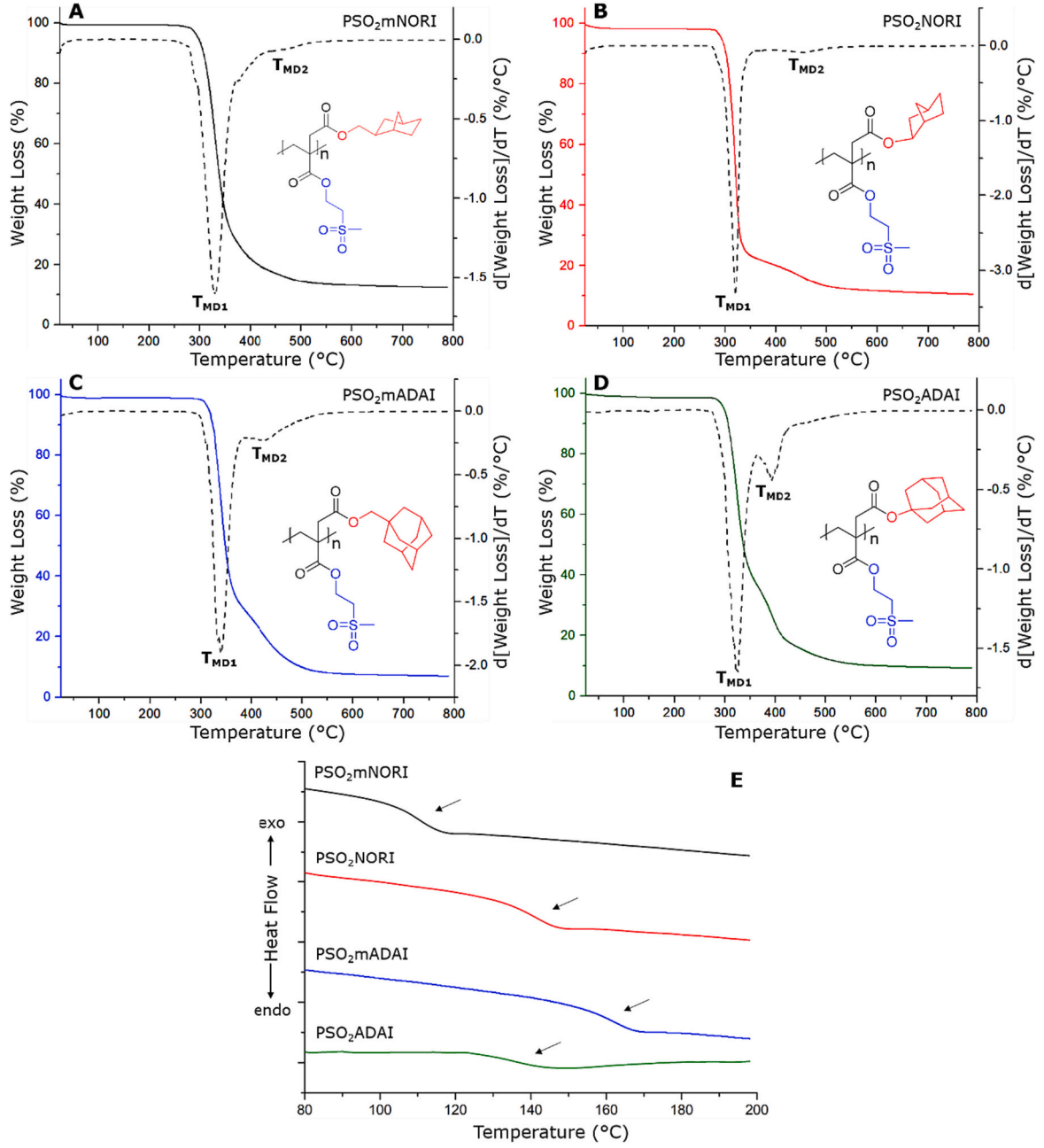

Fig. 3. TGA (A, B, C and D) and DSC (E) thermograms registered for polyitaconates. T_gs are indicated by black arrows.

Table 2
Thermal degradation onset temperature (T_i), maximum weight loss rate temperature (T_{MD}), residue percentage (R) and glass transition temperature for the obtained polyitaconates.

Sample	T_i (°C)	T_{MD1} (°C)	T_{MD2} (°C)	R (%)	T_g (°C)
PSO_2mNORI	299	329	472	12	111
PSO_2NORI	297	320	453	10	143
PSO_2mADAI	319	339	426	7	166
PSO_2ADAI	301	324	392	9	136

observed. These variations in ε_r' can be correlated with ε_r" profiles through diverse relaxation phenomena. In this sense, it can be seen that in all cases, the abrupt increase in ε_r' at low temperatures manifests as a clear peak in the ε_r" profiles (labeled γ), indicating the occurrence of molecular relaxation phenomena.

Drawing on previous dielectric investigations on polymethacrylates and polyitaconates, especially for PSO_2MeiT, this γ relaxation can primarily be attributed to the orientational motions of sulfone entities [20,34,52]. We use "primarily" here, as it has been demonstrated in past reports that both carbonyl species in polyitaconates, acting as dipolar entities in their respective monomeric units, contribute to polarization through different relaxation processes known as β_{FAST} and β_{SLOW} transitions [57]. Carbonyl species separated by a methylene unit from the polymer backbone are responsible for β_{FAST} relaxation, which occurs within the same temperature range as γ relaxation. However, the dielectric strength of these molecular motions is notably lower than that produced by sulfones. Thus, it is reasonable to consider sulfone entities as the main drivers of these γ relaxations and, consequently, of the polarized state exhibited by these materials. Importantly, the maxima of γ relaxations at 1 Hz are centered at −96 °C, − 101 °C, − 98 °C and − 97 °C for PSO_2mNORI, PSO_2NORI, PSO_2mADAI and PSO_2ADAI,

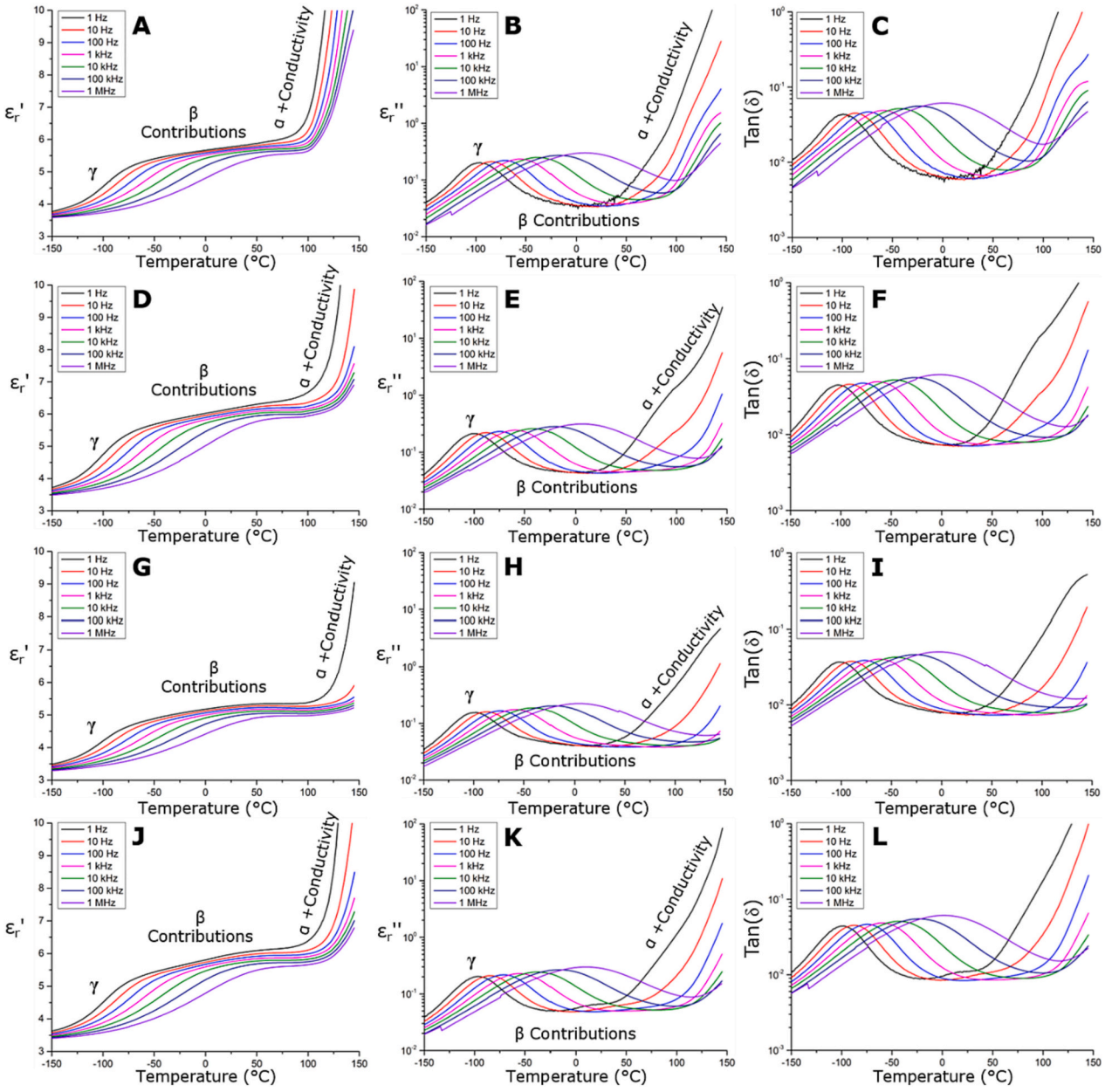

Fig. 4. Isochronal scans of ε_r', ε_r" and Tan(δ) for PSO_2mNORI (A, B, C), PSO_2NORI (D, E, F), PSO_2mADAI (G, H, I) and PSO_2ADAI (J, K, L).

respectively, indicating that sulfone movements are active and thus contribute to polarization from remarkably low temperatures.

Conversely, carbonyl species directly attached to the polymer main chain begin to contribute to their molecular motions (β_{SLOW} transitions) at temperatures above – 50 °C [34,57]. For clarity, in Figs. 4 B, E, H, K β_{FAST} and β_{SLOW} transitions have been grouped together and labeled as β contributions. It is important to note that since γ, β_{FAST} and β_{SLOW} molecular motions occur at temperatures below the T_g, these sub-T_g

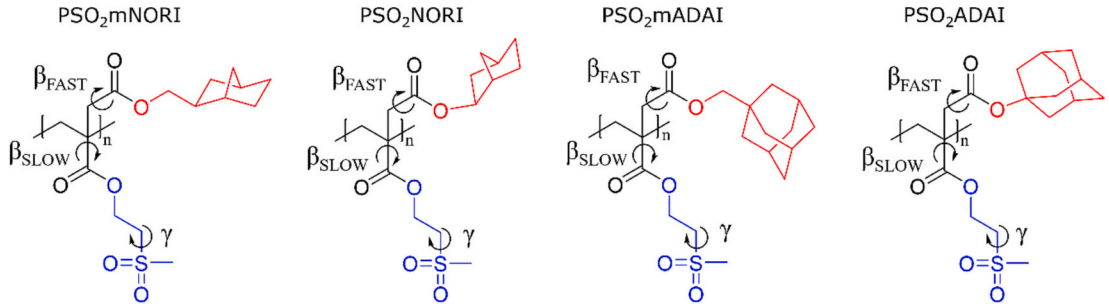

Scheme 3. Assignment of molecular motions to the observed dielectric relaxations in isochronal spectra.

transitions are responsible for the dielectric properties exhibited by these polyitaconates in their *dipolar glass polymer* state. Scheme 3 illustrates the aforementioned transitions along their respective molecular motions.

In contrast, the abrupt increase in ε_r' observed at high temperatures, accompanied by a noticeable increase in ε_r" and Tan(δ), can be attributed to samples entering the *paraelectric* state. This state, which is highly polarized but also highly dissipative, is achieved when the temperature of the system approaches/surpasses its T_g, usually referred to as α relaxation in broadband dielectric spectroscopy. Therefore, in addition to the local movements of dipolar entities, long-segmental motions (e.g., translational) of polymer chains begin to contribute to the polarization of the material.

Regrettably, the same increase in chain mobility that leads to this dramatic rise in polarization (ε_r') also augments the dissipative nature of the material (as seen in ε_r" and Tan(δ)). This can be explained by a rise in internal friction within the system, promoting the dissipation of energy in the form of heat. Simultaneously, it facilitates the diffusion of ionic impurities, which are invariably present, directly impacting the insulating property of the material and thus promoting energy dissipation through conductivity phenomena. These arguments elucidate the necessity of delaying the onset of the *paraelectric* state on the temperature scale. In this context, Fig. 5 A reveals that in all obtained polyitaconates, the abrupt rise of ε_r' has been remarkably displaced toward higher temperatures when compared to the already reported PSO_2MeiT specimen [34]. This indicates an effective delay of the *paraelectric* state and thus dissipative phenomena. Judging by the achieved T_g values, this was an already expected result, supporting the inclusion of these bulky entities as a strategy to expand the range of temperatures where these materials can work properly, with optimal polarization and low dissipative behavior (Fig. 5B). In this regard, the magnitude of the DGP temperature range for each system can be calculated by subtracting the temperature at which the paraelectric state starts contributing ($T_{paraelectric}$) to the temperature at which the maxima of the γ transition occur (T_γ). Table 3 summarizes the above-described temperature values and the range of temperatures in which each system behaves as a DGP, evidencing the superiority of these materials against PSO_2MeiT.

After successfully corroborating the obtained DGPs with markedly increased working temperature ranges, we proceeded by evaluating their ε_r' and Tan(δ) values. As mentioned earlier, both parameters are of utmost importance when envisioning the performance of these materials as potential dielectric layers in capacitor devices. To our delight, ε_r' profiles from Fig. 4 confirm that all these polyitaconates exhibited ε_r' values above 5.0 at 1 Hz and 1 kHz at room temperature, allowing them to be considered formally as high-dielectric polymers. Furthermore, and fortunately, they also registered remarkably low Tan(δ) values – below 0.01 – despite their dipolar nature, thus qualifying as low dissipative materials. Table 4 summarizes the ε_r' and Tan(δ) values, along with other relevant properties useful to delve into the dielectric behavior of these materials.

Further inspection of Table 4 revealed that three of the four polymers exhibited ε_r' values above 5.5 – even exceeding the value of 6.0 in the case of PSO_2NORI – while registering loss factors of approximately 0.007–0.008. In this context, these materials successfully outperformed their nitrile-containing counterparts in terms of dielectric behavior [43], confirming our previous findings on using sulfones as dipolar functionalities when designing superior polyitaconate-based dielectrics [34]. Interestingly, it is evidenced that polymers bearing norbornane structures tend to register increased ε_r' compared to those having adamantane pendant groups. Furthermore, it is also observed that those systems presenting methylene spacer units – PSO_2mNORI and PSO_2mADAI – exhibited lower ε_r' values than their respective relatives. Both results could be argued, to some extent, in terms of the monomeric densities presented by these polymers (Table 4) and how this property is notably affected by the structure and molecular weight of the bulky substituent employed, serving as a direct measurement of the number of dipoles present per volume unit of material. Logically, while not always true, a higher dipolar density gives way to greater polarizability, favoring the attainment of increased ε_r' values. This seems to correlate well with our results, except when comparing PSO_2mNORI and PSO_2ADAI, which registered similar ε_r' values even when showing considerable differences regarding their monomeric densities. This out-of-trend result could be explained considering that the polarization of a dipolar material – and consequently its ε_r' – would depend not only on the number and dipole moment of its dipolar structures but also on the ability of these entities to respond to the external electric field through orientational motions. The latter is critical since it has been demonstrated that only a fraction of dipoles is able to overcome the potential energy barrier imposed by the polymer matrix [20,31,34]. Due to the above, we pursued the theoretical calculation of the dipolar mobility for these materials, aiming to gain a better understanding of their dielectric properties.

The dipolar mobility of sulfones was calculated using our previously reported protocol based on the Onsager formalism (eq. 2) for freely rotating dipolar liquids [34,42,43].

$$\frac{\left[\left(\varepsilon_{Onsager}-\varepsilon_{\infty}\right)\left(2\varepsilon_{Onsager}+\varepsilon_{\infty}\right)\right]}{\left[\varepsilon_{Onsager}\left(\varepsilon_{\infty}+2\right)^{2}\right]}=\frac{N\,\mu^{2}}{9\varepsilon_{o}K_{B}T} \quad (2)$$

Herein, $\varepsilon_{Onsager}$ would be the value arising from the utopian situation where all dipoles (sulfones) contribute to the material's polarization, representing a system with full dipole mobility. On the other hand, ε_∞, N, μ, ε_o, K_B and T are the instantaneous dielectric constant (defined in

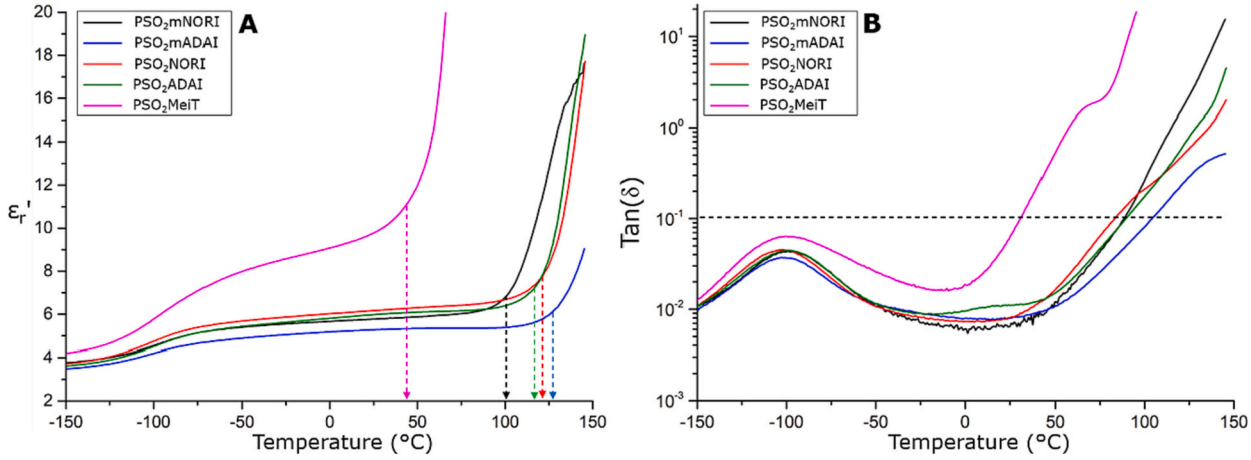

Fig. 5. ε_r' (A) and Tan(δ) (B) profiles registered at 1 Hz for the synthesized polyitaconates and the previously reported PSO_2MeiT.

Table 3
Temperature values extracted from isochronal measurements (1 Hz) and used to determine the DGP's temperature range of polyitaconates.

	PSO_2MeiT[d]	PSO_2mNORI	PSO_2NORI	PSO_2mADAI	PSO_2ADAI
T_γ (°C)[a]	– 96	– 96	– 101	– 98	– 97
$T_{paraelectric}$ (°C)[b]	47	102	124	127	122
DGP's temperature range (°C)[c]	143	198	225	225	220

[a] Obtained from ε_r" isochrones at 1 Hz.
[b] Calculated using the protocol reported in [22].
[c] Calculated as $T_{paraelectric} - T_\gamma$.
[d] Values from reference [34].

Table 4
Dielectric parameters and monomeric density values for the obtained polyitaconates.

	PSO_2mNORI	PSO_2NORI	PSO_2mADAI	PSO_2ADAI
ε_r' (1 Hz, 25 °C)	5.8	6.2	5.3	5.9
ε_r' (1 kHz, 25 °C)	5.6	6.0	5.1	5.7
Tan(δ) (1 Hz, 25 °C)	0.007	0.008	0.008	0.008
ε_r'(1 Hz, – 50 °C)	5.4	5.7	4.9	5.4
$\varepsilon_{electronic}$ [a]	2.3	2.3	2.3	2.3
ε_∞ [b]	2.8	2.8	2.8	2.8
Monomeric density [c]	2.24×10^{27}	2.26×10^{27}	1.91×10^{27}	1.95×10^{27}

[a] Calculated from $n^2 = \varepsilon_{electronic}$ [18].
[b] Calculated using equation $\varepsilon_\infty = \varepsilon_{electronic} + \varepsilon_{atomic}$, considering $\varepsilon_{atomic} = 0.2\ \varepsilon_{electronic}$ [58].
[c] Number of monomer units per m^3 of material.

Table 4), dipolar density (N° of sulfones per m^3), dipole moment (1.42×10^{-29}C m), vacuum permittivity (~ 8.85×10^{-12} F m^{-1}), Boltzmann constant (~ 1.38×10^{-23} m kg s^{-2} K^{-1}) and absolute temperature, respectively. For the calculations, the employed ε_∞ and N values are those presented in Table 4, while for μ, the value was obtained from the dipole moment reported for sulfones in Debye units (4.25 D). Moreover, the temperature selected was 223 K (– 50 °C) based on the inspection of the ε_r" isochrone profiles at 1 Hz, determining that molecular motions of sulfones – γ transitions – are already active and contribute to ε_r'. Therefore, $\varepsilon_{Onsager}$ values of 22.8, 23.0, 19.7 and 20.1 were calculated for PSO_2mNORI, PSO_2NORI, PSO_2mADAI and PSO_2ADAI, respectively, which were used together with the experimental parameter $\varepsilon_r'_{(1\ Hz,\ -\ 50\ °C)}$ (Table 4) to calculate the dipole mobility of sulfones through eq. 3:

$$\text{Dipole mobility } (\%) = \frac{\left(\varepsilon_r'_{(1\ Hz,-50°C)} - \varepsilon_\infty - \varepsilon_{PDMeI}^{dipolar}\right)}{\left(\varepsilon_{Onsager} - \varepsilon_\infty\right)} \text{ x } 100 \quad (3)$$

The presence of ε_∞ and $\varepsilon_{PDMeI}^{dipolar}$ in the above equation allows the suppression of any contribution to $\varepsilon_r'_{(1\ Hz,\ -\ 50\ °C)}$ unrelated to sulfone dipoles. In this context, by subtracting ε_∞, the influence of the electronic and atomic polarization mechanisms is eliminated, while the second term is incorporated to exclude the contributions of carbonyl species present in the polyitaconate backbone. This latter term can be obtained using, as an approximation, the dielectric properties measured for poly (dimethylitaconate) (PDMeI), since its dipolar polarization would be essentially ascribed to the presence of carbonyls. In this regard, we have previously reported the dielectric properties of PDMeI, from which values of 3.59 and 2.69 were registered for $\varepsilon_r'_{(1\ Hz,\ -\ 50\ °C)}$ and ε_∞, respectively [34]. Then, the calculation of $\varepsilon_{PDMeI}^{dipolar}$ is accomplished by subtracting ε_∞ from $\varepsilon_r'_{(1\ Hz,\ -\ 50\ °C)}$, resulting in a value of 0.9. However, as noted above, the dipole-based polarization highly depends on the density of the materials. Thus, in this case, the value of 0.9 was calculated from a PDMeI sample exhibiting a density of 1.29 g/cm^3–4.66 × 10^{27} monomers/m^3 – which differs importantly from the monomeric densities measured for the polyitaconates reported in this work. Therefore, by applying a simple proportional correction that considers the above, $\varepsilon_{PDMeI}^{dipolar}$ values of 0.43, 0.44, 0.37 and 0.38 were calculated and used in eq. 3, through which values of 10.9, 12.2, 10.2 and 12.8% were obtained for PSO_2mNORI, PSO_2NORI, PSO_2mADAI and PSO_2ADAI, respectively. The obtained results show that the average orientational ability of sulfone dipoles is small, yet these fulfill the requirements to be considered high-dielectric polymers. Nevertheless, it must be noted that these mobility values find a good correlation with previous reports on dipole-containing polymers [31,34,42,43].

Importantly, the inclusion of the dipole mobility as a new tool for discussing the dielectric response of these materials allows us to reach a better understanding of the obtained results. For instance, we can now explain the unexpectedly similar ε_r' values registered for PSO_2mNORI and PSO_2ADAI in terms of the higher mobility calculated for the latter that would counterbalance its lower dipole density. Another interesting observation is the higher dipole mobility exhibited by PSO_2NORI and PSO_2ADAI, both specimens sharing the absence of spacer units in the bulky substituents, and therefore, this finding could guide the design of new polymer dielectrics, avoiding the inclusion of these types of fragments. On the other hand, the greater dipole moment of sulfones, together with their notably higher mobility, would also explain the superior performance evidenced by these polyitaconates when compared against their nitrile-bearing versions. In this context, this work supports our previous findings regarding the advantages of using sulfones instead of nitriles as dipolar entities. Likewise, the greater ε_r' value reported for PSO_2MeiT would be ascribed to the slightly higher mobility of their sulfones (15%) but primarily to its markedly higher monomeric density [34]. Nevertheless, as demonstrated above, this specimen lacks a suitable working temperature range, making sense the sacrifice of ε_r' in exchange for gaining better functioning under actual working conditions by introducing these bulky groups. Finally, frequency scans at low temperatures were used to provide a more detailed analysis of the sulfone motions represented by γ relaxations. Therefore, Fig. 6 displays ε_r" isotherm curves registered between – 100 °C and – 20 °C, evidencing in all cases the presence of relaxations correlated to the γ transitions previously detected in isochrone curves. These relaxations expose the typical behavior for sub-T_g transitions assigned to localized molecular motions, showing an intensity increase and shifting toward higher frequencies as the temperature of the system rises. The above argued in terms of the thermal activation that these dipolar entities need to achieve these local movements. In this sense, frequency scans are especially useful for evaluating the dependence of the relaxation times of certain molecular motions on the temperature from which the activation energy (E_a) can be calculated. Thus, by measuring the frequency at which the maxima of the relaxation appear (f_{max}) in ε_r" isotherm scans, the relaxation time for each temperature can be calculated as $\tau_{max} = (2\pi f_{max})^{-1}$. Then, these data are fitted using the linearized form of the Arrhenius equation plotting $\ln(\tau_{max})$ vs 1/T and extracting the E_a value from the slope (insets in Fig. 6) [18].

From the above Arrhenius plots, E_a values of 56.8, 53.0, 59.0 and 56.4 kJ/mol were calculated for PSO_2mNORI, PSO_2NORI, PSO_2mADAI and PSO_2ADAI, respectively. Even when all these values fall within the same order of magnitude, their subtle differences could find a good correlation to the dielectric response shown by each sample. In this context, it is interesting to note the inverse relation observed between E_a and ε_r' for these materials. This means that the samples with higher ε_r'

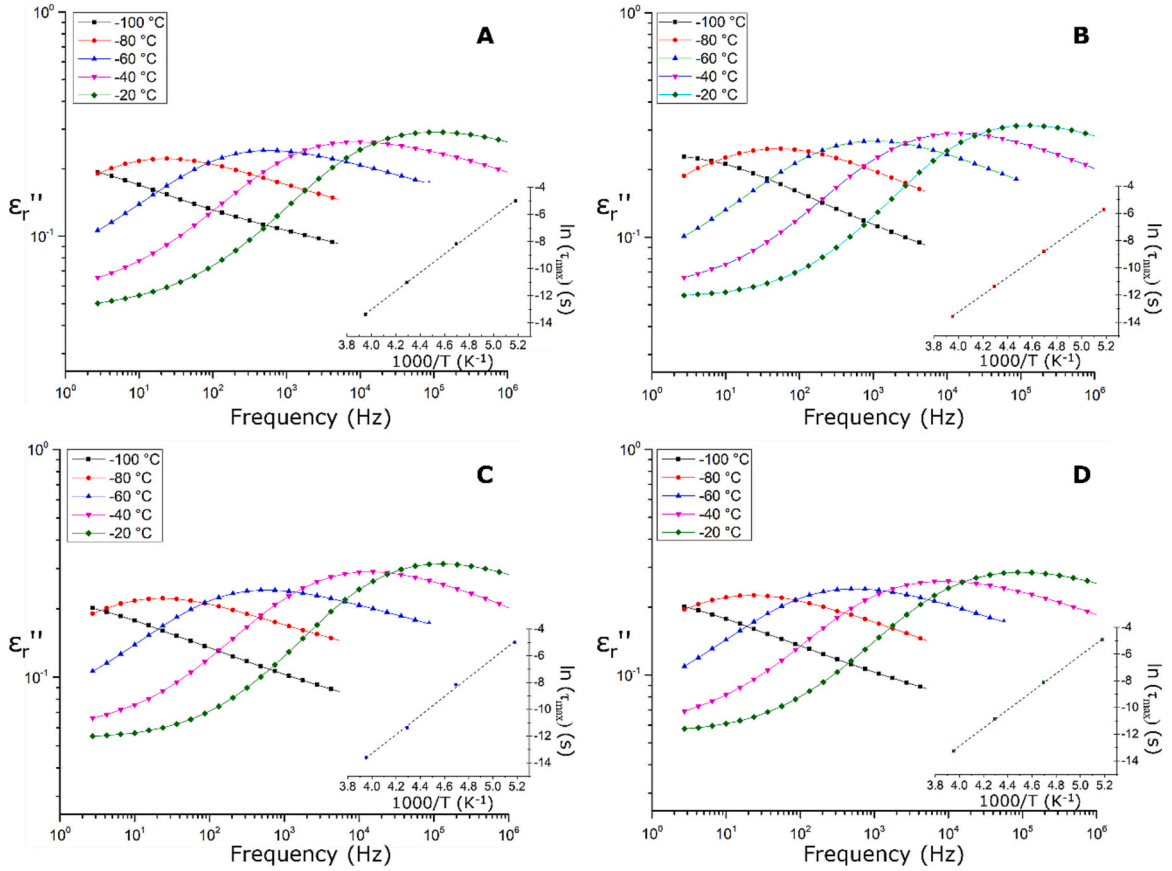

Fig. 6. ε_r'' frequency scans registered at low temperatures for PSO_2mNORI (A), PSO_2NORI (B), PSO_2mADAI (C) and PSO_2ADAI (D). Insets: Linear fits of Arrhenius plots.

values also exhibit lower E_a, and vice versa. For example, the lowest E_a belongs to PSO_2NORI, which also shows the highest ε_r', primarily due to its greater dipole mobility. This suggests that the higher dipole mobility of PSO_2NORI may, to some extent, be related to its lower E_a, indicating a less restrictive environment for dipole motions provided by this material. The same reasoning can be applied to the other samples. Interestingly, and similar to our previous findings, it seems that the incorporation of methylene spacer units increases E_a. Therefore, the better packing allowed for the adamantane and norbornane structures separated from the polymer backbone by these spacer units are likely to provide a more hindering environment for dipole orientations. In any case, the E_a values calculated for sulfones present in this new family of polyitaconates are considerably lower than those calculated for carbonyl structures of polymethacrylates, which are considered entities with adequate mobility [55].

4. Conclusions

In conclusion, we have successfully prepared and characterized four new polyitaconates exhibiting adequate thermal and dielectric properties for energy storage applications. The employed strategy consisted of taking advantage of the dual functionality offered by the itaconate monomer. This allowed us to combine different functionalities in one single material, each responsible for enhancing one of the properties separately. On the one hand, the inclusion of sulfones as high dipole moment entities allowed the achievement of materials exhibiting high ε_r' values, ranging between 5.1 and 6.2. This notably surpasses the typical values shown by conventional polymers while maintaining relatively low Tan(δ) values. As a result, they can be classified as high-dielectric polymers with low dissipative behavior. On the other hand, the simultaneous incorporation of norbornane and adamantane derivatives proved to be an effective strategy for improving the thermal properties of these materials and, consequently, their dissipative behavior. In this regard, samples exhibited decomposition onset temperatures well above 250 °C and T_g values ranging between 111 °C and 166 °C. Due to these effects, these materials delay their transitions into the *paraelectric* state on the temperature scale. Consequently, they also delay the early appearance of dissipative phenomena, expanding the range of temperatures at which these systems can operate while maintaining a high polarized state and low energy dissipation. This work provides additional support for our previous efforts in proposing polyitaconates as suitable dielectric materials. This demonstrates that this class of sustainable materials, when accompanied by proper chemical design, can meet the basic requirements for applications in diverse high-tech fields and, especially, as improved polymer dielectrics in capacitor devices.

CRediT authorship contribution statement

Sebastian Bonardd: Writing – original draft, Visualization, Supervision, Methodology, Investigation, Formal analysis, Data curation, Conceptualization. **Jon Maiz:** Writing – original draft, Funding acquisition. **Angel Alegría:** Writing – original draft, Investigation, Funding acquisition. **José A. Pomposo:** Writing – original draft, Funding acquisition. **Ester Verde Sesto:** Funding acquisition. **Galder Kortaberria:** Resources, Funding acquisition. **David Díaz Díaz:** Writing – original draft, Resources, Funding acquisition.

Declaration of competing interest

The authors declare that they have no known competing financial interests or personal relationships that could have appeared to influence

the work reported in this paper.

Data availability

Data will be made available on request.

Acknowledgments

The Polymers & Soft Matter team acknowledges the funding provided by Grant No. PID2021-123438NB-I00 from MCIN/AEI/10.13039/501100011033, as well as the support from "ERDF A way of making Europe," Grant No. TED2021-130107 A-I00, also funded by MCIN/AEI/10.13039/501100011033, and Unión Europea "NextGenerationEU/PRTR." Additionally, we acknowledge the financial support from Eusko Jaurlaritza under code: IT1566-22 and Gipuzkoako Foru Aldundia, Programa de Red Guipuzcoana de Ciencia,

Tecnología e Innovación, code: 2023-CIEN-000069-01. G. K. thanks to Ministerio de Ciencia, Innovacion y Universidades, grant number PID2021-126417NB-I00 and by the Gobierno Vasco/Eusko Jaurlaritza, grant number IT1690-22. D. D. D. thanks the Spanish Ministry of Science, Innovation and Universities for the grants TED2021-132847B-I00 and PID2019-105391GB-C21 funded by MCIN/AEI/10.13039/501100011033 and NANOtec, INTech, Cabildo de Tenerife and ULL for laboratory facilities.

Appendix A. Supplementary data

Supplementary data to this article can be found online at https://doi.org/10.1016/j.reactfunctpolym.2024.105842.

References

[1] B. Fan, M. Zhou, C. Zhang, D. He, J. Bai, Polymer-based materials for achieving high energy density film capacitors, Prog. Polym. Sci. 97 (2019) 101143.
[2] Z. Zhang, J. Zheng, K. Premasiri, M.-H. Kwok, Q. Li, R. Li, S. Zhang, M.H. Litt, X.P. A. Gao, L. Zhu, High-κ polymers of intrinsic microporosity: a new class of high temperature and low loss dielectrics for printed electronics, Mater. Horizons. 7 (2020) 592–597.
[3] E. Baer, L. Zhu, 50th anniversary perspective: dielectric phenomena in polymers and multilayered dielectric films, Macromolecules. 50 (2017) 2239–2256, https://doi.org/10.1021/acs.macromol.6b02669.
[4] Y. Qiao, X. Yin, T. Zhu, H. Li, C. Tang, Dielectric polymers with novel chemistry, compositions and architectures, Prog. Polym. Sci. 80 (2018) 153–162.
[5] J. Wei, L. Zhu, Intrinsic polymer dielectrics for high energy density and low loss electric energy storage, Prog. Polym. Sci. 101254 (2020).
[6] Q.K. Feng, S.L. Zhong, J.Y. Pei, Y. Zhao, D.L. Zhang, D.F. Liu, Y.X. Zhang, Z. M. Dang, Recent Progress and future prospects on all-organic polymer dielectrics for energy storage Capacitors, Chem. Rev. 122 (2022) 3820–3878, https://doi.org/10.1021/acs.chemrev.1c00793.
[7] X. Wu, X. Chen, Q.M. Zhang, D.Q. Tan, Advanced dielectric polymers for energy storage, Energy Storage Mater. 44 (2022) 29–47, https://doi.org/10.1016/j.ensm.2021.10.010.
[8] S. Wang, C. Yang, X. Li, H. Jia, S. Liu, X. Liu, T. Minari, Q. Sun, Polymer-based dielectrics with high permittivity and low dielectric loss for flexible electronics, J. Mater. Chem. C 10 (2022) 6196–6221.
[9] A. Mannodi-Kanakkithodi, T.D. Huan, R. Ramprasad, Mining materials design rules from data: the example of polymer dielectrics, Chem. Mater. 29 (2017) 9001–9010, https://doi.org/10.1021/acs.chemmater.7b02027.
[10] A. Mannodi-Kanakkithodi, G. Pilania, T.D. Huan, T. Lookman, R. Ramprasad, Machine learning strategy for accelerated design of polymer dielectrics, Sci. Rep. 6 (2016) 20952.
[11] R. Wang, Y. Zhu, J. Fu, M. Yang, Z. Ran, J. Li, M. Li, J. Hu, J. He, Q. Li, Designing tailored combinations of structural units in polymer dielectrics for high-temperature capacitive energy storage, Nat. Commun. 14 (2023) 2406.
[12] S. Zhang, R. Shinwari, S. Zhao, Energy transition, geopolitical risk, and natural resources extraction: a novel perspective of energy transition and resources extraction, Resour. Policy. 83 (2023) 103608.
[13] S. Nasreen, G.M. Treich, M.L. Baczkowski, A.K. Mannodi-Kanakkithodi, Y. Cao, R. Ramprasad, G. Sotzing, Polymer dielectrics for capacitor application, Kirk-Othmer Encycl. Chem. Technol. 1–29 (2000).
[14] D. Butnicu, A. Lazar, Why Choose Polymer Electrolytic Output Capacitors for Maximum Ripple Capability and Reliability Performance within eGaN based POL Converters, EPE 2020 - Proc. 2020 11th Int. Conf. Expo. Electr. Power Eng, 2020, pp. 12–15, https://doi.org/10.1109/EPE50722.2020.9305652.
[15] G. Zhang, Q. Li, E. Allahyarov, Y. Li, L. Zhu, Challenges and opportunities of polymer Nanodielectrics for capacitive energy storage, ACS Appl. Mater. Interfaces 13 (2021) 37939–37960, https://doi.org/10.1021/acsami.1c04991.
[16] Q. Li, F.-Z. Yao, Y. Liu, G. Zhang, H. Wang, Q. Wang, High-temperature dielectric materials for electrical energy storage, Annu. Rev. Mat. Res.48 (2018) 219–243.
[17] L. Zhu, Exploring strategies for high dielectric constant and low loss polymer dielectrics, J. Phys. Chem. Lett. 5 (2014) 3677–3687, https://doi.org/10.1021/jz501831q.
[18] C.C. Ku, R. Liepins, Electrical Properties of Polymers—Chemical Principles, Carl Hanser, 1988.
[19] T. Blythe, D. Bloor, Electrical Properties of Polymers, Cambridge University Press, 2005, https://doi.org/10.2277/0521552192.
[20] J. Wei, Z. Zhang, J.-K. Tseng, I. Treufeld, X. Liu, M.H. Litt, L. Zhu, Achieving high dielectric constant and low loss property in a dipolar glass polymer containing strongly dipolar and small-sized sulfone groups, ACS Appl. Mater. Interfaces 7 (2015) 5248–5257, https://doi.org/10.1021/am508488w.
[21] S. Bonardd, V. Moreno-Serna, G. Kortaberria, D. Díaz Díaz, A. Leiva, C. Saldías, Dipolar glass polymers containing polarizable groups as dielectric materials for energy storage applications. A minireview, Polymers (Basel). 11 (2019) 317.
[22] S. Bonardd, Á. Alegria, C. Saldías, Á. Leiva, G. Kortaberria, Increasing the temperature range of dipolar glass polymers through copolymerization: a first approach to dipolar glass copolymers, Polymer (Guildf). 203 (2020) 122765.
[23] H. Luo, F. Wang, R. Guo, D. Zhang, G. He, S. Chen, Q. Wang, Progress on polymer dielectrics for electrostatic Capacitors application, Adv. Sci. 9 (2022) 1–25, https://doi.org/10.1002/advs.202202438.
[24] J. Qiu, Q. Gu, Y. Sha, Y. Huang, M. Zhang, Z. Luo, Preparation and application of dielectric polymers with high permittivity and low energy loss: a mini review, J. Appl. Polym. Sci. 139 (2022) 1–18, https://doi.org/10.1002/app.52367.
[25] H. Xu, S. Chen, S. Chen, R. Qiao, H. Li, H. Luo, D. Zhang, Constructing high-performance dielectrics via molecular and phase engineering in dipolar polymers, ACS Appl. Energy Mater. 4 (2021) 2451–2462, https://doi.org/10.1021/acsaem.0c02962.
[26] H. Luo, C. Yan, X. Liu, H. Luo, S. Chen, Constructing novel high-performance dipolar glass polymer dielectrics by polar rigid/flexible side chains, ACS Appl. Mater. Interfaces15 (2023) 24470–24482.
[27] X. Tang, C. Din, S. Yu, Y. Liu, H. Luo, D. Zhang, S. Chen, Synthesis of dielectric polystyrene via one-step nitration reaction for large-scale energy storage, Chem. Eng. J. 446 (2022) 137281, https://doi.org/10.1016/j.cej.2022.137281.
[28] D.H. Wang, B.A. Kurish, I. Treufeld, L. Zhu, L. Tan, Synthesis and characterization of high nitrile content polyimides as dielectric films for electrical energy storage, J. Polym. Sci. Part A Polym. Chem. 53 (2015) 422–436.
[29] F. Owusu, M. Tress, F.A. Nüesch, S. Lehner, D.M. Opris, Synthesis of polar polynorbornenes with high dielectric relaxation strength as candidate materials for dielectric applications, Mater. Adv. 3 (2022) 998–1006.
[30] S. Bonardd, E. Robles, I. Barandiaran, C. Saldías, Á. Leiva, G. Kortaberria, Biocomposites with increased dielectric constant based on chitosan and nitrile-modified cellulose nanocrystals, Carbohydr. Polym. 199 (2018) 20–30.
[31] J.T. Bendler, D.A. Boyles, C.A. Edmondson, T. Filipova, J.J. Fontanella, M. A. Westgate, M.C. Wintersgill, Dielectric properties of bisphenol a polycarbonate and its tethered nitrile analogue, Macromolecules. 46 (2013) 4024–4033.
[32] J. Liu, M. Li, Y. Zhao, X. Zhang, J. Lu, Z. Zhang, Manipulating H-bonds in glassy dipolar polymers as a new strategy for high energy storage capacitors with high pulse discharge efficiency, J. Mater. Chem. A 7 (2019) 19407–19414.
[33] C. Wang, Z. Zhang, S. Pejić, R. Li, M. Fukuto, L. Zhu, G. Sauvé, High dielectric constant semiconducting poly (3-alkylthiophene) s from side chain modification with polar sulfinyl and sulfonyl groups, Macromolecules. 51 (2018) 9368–9381.
[34] S. Bonardd, A. Alegria, C. Saldias, A. Leiva, G. Kortaberria, Polyitaconates: a new family of "all-polymer" dielectrics, ACS Appl. Mater. Interfaces 10 (2018) 38476–38492.
[35] S.J. Dünki, E. Cuervo-Reyes, D.M. Opris, A facile synthetic strategy to polysiloxanes containing sulfonyl side groups with high dielectric permittivity, Polym. Chem. 8 (2017) 715–724.
[36] H. Tong, J. Fu, A. Ahmad, T. Fan, Y. Hou, J. Xu, Sulfonyl-containing polyimide dielectrics with advanced heat resistance and dielectric properties for high-temperature capacitor applications, Macromol. Mater. Eng. 304 (2019) 1800709.
[37] Z. Zhang, D.H. Wang, M.H. Litt, L. Tan, L. Zhu, High-temperature and high-energy-density dipolar glass polymers based on sulfonylated poly (2, 6-dimethyl-1, 4-phenylene oxide), Angew, Chemie. 130 (2018) 1544–1547.
[38] Y.F. Zhu, Z. Zhang, M.H. Litt, L. Zhu, High dielectric constant sulfonyl-containing dipolar glass polymers with enhanced Orientational polarization, Macromolecules. (2018), https://doi.org/10.1021/acs.macromol.8b00923.
[39] W. Huang, T. Ju, R. Li, Y. Duan, Y. Duan, J. Wei, L. Zhu, High-κ and high-temperature dipolar glass polymers based on Sulfonylated and Cyanolated poly (Arylene ether)s for capacitive energy storage, Adv. Electron. Mater. 9 (2023), https://doi.org/10.1002/aelm.202200414.
[40] H. Xu, G. He, S. Chen, S. Chen, R. Qiao, H. Luo, D. Zhang, All-organic polymer dielectrics containing sulfonyl dipolar groups and π-πStacking interaction in side-chain architectures, Macromolecules. 54 (2021) 8195–8206, https://doi.org/10.1021/acs.macromol.1c00778.
[41] J. Wei, T. Ju, W. Huang, J. Song, N. Yan, F. Wang, A. Shen, Z. Li, L. Zhu, High dielectric constant dipolar glass polymer based on sulfonylated poly (ether ether ketone), Polymer (Guildf). 178 (2019) 121688.
[42] S. Bonardd, Á. Alegria, C. Saldías, Á. Leiva, G. Kortaberria, Synthesis of new poly (itaconate) s containing nitrile groups as high dipolar moment entities for the development of dipolar glass polymers with increased dielectric constant. Thermal and dielectric characterization, Eur. Polym. J. 114 (2019) 19–31.

[43] S. Bonardd, Á. Alegria, O. Ramirez, C. Saldías, Á. Leiva, G. Kortaberria, New poly (itaconate) s with bulky pendant groups as candidates for "all-polymer" dielectrics, React. Funct. Polym. 140 (2019) 1–13.
[44] B. Neises, W. Steglich, Simple method for the esterification of carboxylic acids, Angew. Chemie Int. Ed. English. 17 (1978) 522–524.
[45] A. Matsumoto, H. Watanabe, T. Otsu, Synthesis and radical polymerization of itaconates containing an adamantyl ester group, Bull. Chem. Soc. Jpn. 65 (1992) 846–852.
[46] A. Matsumoto, S. Tanaka, T. Otsu, Synthesis and characterization of poly (1-adamantyl methacrylate): effects of the adamantyl group on radical polymerization kinetics and thermal properties of the polymer, Macromolecules. 24 (1991) 4017–4024.
[47] W. Lei, T.P. Russell, L. Hu, X. Zhou, H. Qiao, W. Wang, R. Wang, L. Zhang, Pendant chain effect on the synthesis, characterization, and structure–property relations of poly (di-n-alkyl itaconate-co-isoprene) biobased elastomers, ACS Sustain. Chem. Eng. 5 (2017) 5214–5223.
[48] N. Tsuji, Y. Suzuki, A. Matsumoto, Adamantane-containing poly (dialkyl fumarate) s with rigid chain structures, Polym. J. 51 (2019) 1147–1161.
[49] R.C. Fort, P.R. Schleyer, Adamantane: consequences of the diamondoid structure, Chem. Rev. 64 (1964) 277–300.
[50] S. Fujii, T.J. McCarthy, Sulfone-containing methacrylate homopolymers: wetting and thermal properties, Langmuir. 32 (2016) 765–771.
[51] F. López-Carrasquero, A.M. de Ilarduya, M. Cárdenas, M. Carrillo, M.L. Arnal, E. Laredo, C. Torres, B. Méndez, A.J. Müller, New comb-like poly (n-alkyl itaconate) s with crystalizable side chains, Polymer (Guildf). 44 (2003) 4969–4979.
[52] S. Bonardd, C. Saldías, Á. Leiva, D. Díaz Díaz, G. Kortaberria, Molecular weight enables fine-tuning the thermal and dielectric properties of polymethacrylates bearing sulfonyl and nitrile groups as dipolar entities, Polymers (Basel). 13 (2021) 317.
[53] P.R. Couchman, A theory of the molecular-mass dependence of glass transition temperatures for polydisperse homopolymers, J. Mater. Sci. 15 (1980) 1680–1683.
[54] K. Fuchise, M. Sone, Y. Miura, R. Sakai, A. Narumi, S.-I. Sato, T. Satoh, T. Kakuchi, Precise synthesis of poly (1-adamantyl methacrylate) by atom transfer radical polymerization, Polym. J. 42 (2010) 626–631.
[55] N. McCrum, B. Read, G. Williams, Anelastic and Dielectric Effects in Polymeric Solids, Wiley Subscription Services, Inc., A Wiley Company, New York, 1967.
[56] J.P. Runt, J.J. Fitzgerald, Dielectric Spectroscopy of Polymeric Materials, American Chemical Society, 1997.
[57] A.-C. Genix, F. Lauprêtre, Subglass and glass transitions of poly (di-n-alkylitaconate) s with various side-chain lengths: dielectric relaxation investigation, Macromolecules. 38 (2005) 2786–2794.
[58] I. Treufeld, D.H. Wang, B.A. Kurish, L.-S. Tan, L. Zhu, Enhancing electrical energy storage using polar polyimides with nitrile groups directly attached to the main chain, J. Mater. Chem. A 2 (2014) 20683–20696.